Research Article | Vol. 25, No. 2 | 23 Jan 2017 | OPTICS EXPRESS 1452
Optics EXPRESS

High-power Yb:GGG thin-disk laser oscillator: first demonstration and power-scaling prospects

A. DIEBOLD,[1,*] Z. JIA,[2,3] I. J. GRAUMANN,[1] Y. YIN,[2] F. EMAURY,[1] C. J. SARACENO,[1] X. TAO,[2] AND U. KELLER[1]

[1]*Institute for Quantum Electronics, ETH Zurich, Zurich, Switzerland*
[2]*State Key Laboratory of Crystal Materials, Shandong University, Ji'nan, China*
[3]*z.jia@sdu.edu.cn*
[*]*diebold@phys.ethz.ch*

Abstract: We present the first demonstration of a thin-disk laser based on the gain material Yb:GGG. This material has many desirable properties for the thin-disk geometry: a high thermal conductivity, which is nearly independent of the doping concentration, a low quantum defect, low-temperature growth, and a broadband absorption spectrum, making it a promising contender to the well-established Yb:YAG for high-power applications. In continuous wave laser operation, we demonstrate output powers above 50 W, which is an order of magnitude higher than previously achieved with this material in the bulk geometry. We compare this performance with an Yb:YAG disk under identical pumping conditions and find comparable output characteristics (with typical optical-to-optical slope efficiencies >66%). Additionally, with the help of finite-element-method simulations, we show the advantageous heat-removal capabilities of Yb:GGG compared to Yb:YAG, resulting in >50% lower thermal lensing for thin Yb:GGG disks compared to Yb:YAG disks. The equivalent optical performance of the two crystals in combination with the easy growth and the significant thermal benefits of Yb:GGG show the large potential of future high-power thin-disk amplifiers and lasers based on this material, both for industrial and scientific applications.

OCIS codes: (140.0140) Lasers and laser optics; (140.3380) Laser materials; (140.3480) Lasers, diode-pumped; (140.3580) Lasers, solid-state; (140.3615) Lasers, ytterbium; (140.6810) Thermal effects.

References and links

1. P. Lacovara, H. K. Choi, C. A. Wang, R. L. Aggarwal, and T. Y. Fan, "Room-temperature diode-pumped Yb:YAG laser," Opt. Lett. **16**(14), 1089–1091 (1991).
2. C. Kränkel, "Rare-earth doped sesquioxides for diode-pumped high power lasers in the 1-, 2-, and 3-µm spectral range," IEEE J. Sel. Top. Quant. Electron. **21**, 1602013 (2015).
3. A. Ellens, H. Andres, M. L. H. ter Heerdt, R. T. Wegh, A. Meijerink, and G. Blasse, "Spectral-line-broadening study of the trivalent lanthanide-ion series. II. The variation of the electron-phonon coupling strength through the series," Phys. Rev. B **55**(1), 180–186 (1997).
4. M. N. Zervas and D. A. Codemard, "High power fiber lasers: a review," IEEE J. Sel. Top. Quantum Electron. **20**(5), 0904123 (2014).
5. P. Russbueldt, D. Hoffmann, M. Hoefer, J. Loehring, J. Luttmann, A. Meissner, J. Weitenberg, M. Traub, T. Sartorius, D. Esser, R. Wester, P. Loosen, and R. Poprawe, "Innoslab Amplifiers," IEEE J. Sel. Top. Quantum Electron. **21**(1), 3100117 (2015).
6. A. Giesen, H. Hügel, A. Voss, K. Wittig, U. Brauch, and H. Opower, "Scalable concept for diode-pumped high-power solid-state lasers," Appl. Phys. B **58**(5), 365–372 (1994).
7. V. Kuhn, T. Gottwald, C. Stolzenburg, S.-S. Schad, A. Killi, and T. Ryba, "Latest advances in high brightness disk lasers," Proc. SPIE **9342**, 93420Y (2015).
8. Boeing, "30 kW multi thin disk laser," *http://boeing.mediaroom.com/Boeing-Thin-Disk-Laser-Exceeds-Performance-Requirements-During-Testing*, retrieved on 2016/11/24 (2013).
9. J.-P. Negel, A. Loescher, A. Voss, D. Bauer, D. Sutter, A. Killi, M. A. Ahmed, and T. Graf, "Ultrafast thin-disk multipass laser amplifier delivering 1.4 kW (4.7 mJ, 1030 nm) average power converted to 820 W at 515 nm and 234 W at 343 nm," Opt. Express **23**(16), 21064–21077 (2015).

#282016 http://dx.doi.org/10.1364/OE.25.001452
Journal © 2017 Received 1 Dec 2016; revised 11 Jan 2017; accepted 12 Jan 2017; published 19 Jan 2017

Optics EXPRESS

10. IFSW, "Thin-disk multipass amplifier," *http://www.ifsw.uni-stuttgart.de/artikel/art16_04.html?__locale=en*, retrieved on 2016/11/16 (2016).
11. M. Schultze, S. Klingebiel, C. Wandt, C. Y. Teisset, R. Bessing, M. Haefner, S. Prinz, K. Michel, and T. Metzger, "500 W - 10 mJ - picosecond thin-disk regenerative amplifier," in *Europhoton Conference* (2016), paper SSL-5.4.
12. M. Ueffing, R. Lange, T. Pleyer, V. Pervak, T. Metzger, D. Sutter, Z. Major, T. Nubbemeyer, and F. Krausz, "Direct regenerative amplification of femtosecond pulses to the multimillijoule level," Opt. Lett. **41**(16), 3840–3843 (2016).
13. C. J. Saraceno, F. Emaury, C. Schriber, A. Diebold, M. Hoffmann, M. Golling, T. Suedmeyer, and U. Keller, "Toward millijoule-level high-power ultrafast thin-disk oscillators," IEEE J. Sel. Top. Quantum Electron. **1**, 1100318 (2015).
14. F. Emaury, A. Diebold, A. Klenner, C. J. Saraceno, S. Schilt, T. Südmeyer, and U. Keller, "Frequency comb offset dynamics of SESAM modelocked thin disk lasers," Opt. Express **23**(17), 21836–21856 (2015).
15. J. Brons, V. Pervak, D. Bauer, D. Sutter, O. Pronin, and F. Krausz, "Powerful 100-fs-scale Kerr-lens mode-locked thin-disk oscillator," Opt. Lett. **41**(15), 3567–3570 (2016).
16. C. Stewen, K. Contag, M. Larionov, A. Giesen, and H. Hugel, "A 1-kW CW thin disc laser," IEEE J. Sel. Top. Quantum Electron. **6**(4), 650–657 (2000).
17. S. Radmard, S. Arabgari, and M. Shayganmanesh, "Optimization of Yb:YAG thin-disk-laser design parameters considering the pumping-light back-reflection," Opt. Laser Technol. **63**, 148–153 (2014).
18. M. Javadi-Dashcasan, F. Hajiesmaeilbaigi, H. Razzaghi, M. Mahdizadeh, and M. Moghadam, "Optimizing the Yb:YAG thin disc laser design parameters," Opt. Commun. **281**(18), 4753–4757 (2008).
19. R. Gaumé, B. Viana, D. Vivien, J.-P. Roger, and D. Fournier, "A simple model for the prediction of thermal conductivity in pure and doped insulating crystals," Appl. Phys. Lett. **83**(7), 1355–1357 (2003).
20. K. S. Wentsch, B. Weichelt, L. Zheng, J. Xu, M. A. Ahmed, and T. Graf, "Continuous-wave Yb-doped Sc2SiO5 thin-disk laser," Opt. Lett. **37**(1), 37–39 (2012).
21. K. S. Wentsch, B. Weichelt, S. Günster, F. Druon, P. Georges, M. A. Ahmed, and T. Graf, "Yb:CaF2 thin-disk laser," Opt. Express **22**(2), 1524–1532 (2014).
22. B. Weichelt, M. Rumpel, A. Voss, A. Gross, V. Wesemann, D. Rytz, M. A. Ahmed, and T. Graf, "Yb:YAl3(BO3)4 as gain material in thin-disk oscillators: demonstration of 109 W of IR output power," Opt. Express **21**(22), 25708–25714 (2013).
23. K. Beil, S. T. Fredrich-Thornton, F. Tellkamp, R. Peters, C. Kränkel, K. Petermann, and G. Huber, "Thermal and laser properties of Yb:LuAG for kW thin disk lasers," Opt. Express **18**(20), 20712–20722 (2010).
24. S. Chénais, F. Druon, F. Balembois, P. Georges, A. Brenier, and G. Boulon, "Diode-pumped Yb:GGG laser: comparison with Yb:YAG," Opt. Mater. **22**(2), 99–106 (2003).
25. J. Dong, M. Bass, Y. Mao, P. Deng, and F. Gan, "Dependence of the Yb3+ emission cross section and lifetime on temperature and concentration in yttrium aluminum garnet," J. Opt. Soc. Am. B **20**(9), 1975–1979 (2003).
26. F. D. Patel, E. C. Honea, J. Speth, S. A. Payne, R. Hutcheson, and R. Equall, "Laser demonstration of Yb3Al5O12 (YbAG) and materials properties of highly doped Yb:YAG," IEEE J. Quantum Electron. **37**(1), 135–144 (2001).
27. almazoptics, "*http://www.almazoptics.com/GGG.html*, retrieved on 2016/10/11," (2016).
28. LaserComponents, "*https://www.lasercomponents.com/de/?embedded=1&file=fileadmin/user_upload/home/Datasheets/divers-optik/laserstaebe_kristalle/yb-yag.pdf&no_cache=1*, retrieved on 2016/10/11," (2016).
29. J. Petit, B. Viana, P. Goldner, J.-P. Roger, and D. Fournier, "Thermomechanical properties of Yb3+ doped laser crystals: Experiments and modeling," J. Appl. Phys. **108**(12), 123108 (2010).
30. J. Liu, X. Chen, W. Han, Q. Dai, K. Wu, and H. Zhang, "Generation of 2.6-mJ 400-kW pulses from a compact Yb:Gd3Ga5O12 laser repetitively Q-switched by an acousto-optic modulator," Opt. Express **21**(22), 26605–26611 (2013).
31. Y. Guyot, H. Canibano, C. Goutaudier, A. Novoselov, A. Yoshikawa, T. Fukuda, and G. Boulon, "Yb3+-doped Gd3Ga5O12 garnet single crystals grown by the micro-pulling down technique for laser application. Part 1: Spectroscopic properties and assignment of energy levels," Opt. Mater. **27**(11), 1658–1663 (2005).
32. K. Contag, M. Karszewski, C. Stewen, A. Giesen, and H. Hugel, "Theoretical modelling and experimental investigations of the diode-pumped thin-disk Yb:YAG laser," Quantum Electron. **29**(8), 697–703 (1999).
33. S. Chenais, F. Balembois, F. Druon, G. Lucas-Leclin, and P. Georges, "Thermal lensing in diode-pumped ytterbium lasers - Part I: Theoretical analysis and wavefront measurements," IEEE J. Quantum Electron. **40**(9), 1217–1234 (2004).
34. T. Y. Fan, "Heat Generation in Nd:YAG and Yb:YAG," IEEE J. Quantum Electron. **29**(6), 1457–1459 (1993).
35. J. Shang, X. Zhu, and G. Zhu, "Analytical approach to thermal lensing in end-pumped Yb:YAG thin-disk laser," Appl. Opt. **50**(32), 6103–6120 (2011).
36. H. Yang, K. Zhang, Z. Cai, G. Feng, Y. Wei, and S. Zhou, "Thermal effects in kW Nd:YAG thin disk laser," in *Photonics and Optoelectronics* (SOPO, 2010).
37. S. Chenais, F. Balembois, F. Druon, G. Lucas Leclin, and P. Georges, "Thermal lensing in diode-pumped ytterbium lasers - part II: evaluation of quantum efficiencies and thermo-optic coefficients," IEEE J. Quantum Electron. **40**(9), 1235–1243 (2004).

Optics EXPRESS

38. D. Fagundes-Peters, N. Martynyuk, K. Lunstedt, V. Peters, K. Petermann, G. Huber, S. Basun, V. Laguta, and A. Hofstaetter, "High quantum efficiency YbAG-crystals," J. Lumin. **125**(1-2), 238–247 (2007).

1. Introduction

Increasing the power available from diode-pumped solid-state lasers continues to be a hot topic for both industrial and scientific applications. Reaching high power requires gain materials with excellent thermal properties as well as optimized heat-removal schemes. Most important progress in this area was triggered by the pioneering experiments on laser operation of Yb:YAG [1]. Yb^{3+}(Yb-)doped gain materials have many spectroscopic advantages for high-power operation [2]. They exhibit a small quantum defect, which results in inherently excellent thermal management. Their simple two-manifold energy level structure avoids detrimental loss processes like up conversion, cross relaxation, and excited-state absorption. Combined with the host material YAG, the relatively strong coupling of the electronic 4f-4f transitions to the phonons of the host lattice leads to broad absorption lines between 920 nm and 980 nm [3]. This enables optical pumping with cost-efficient high-power laser-diode arrays and requires no additional external wavelength stabilization. With all these favorable properties Yb-doped materials have been at the forefront of most high-power continuous wave (cw) laser developments achieved in the last decades. Fiber [4], slab [5], and thin-disk [6] geometries have been used to push the available frontiers to previously unimaginable levels.

Among these technologies, thin-disk lasers [6] are particularly well suited for applications requiring excellent spatial and spectral beam quality. In this geometry, the gain medium is shaped as a disk with typical apertures of >1 cm and thickness in the order of 100 µm and used in reflection inside the cavity. The short gain length and therefore low single-pass pump absorption is compensated with a multi-pass pumping scheme. The large spot size versus thickness results in a quasi-1-D heat flow and extremely reduced thermal aberrations, which enables power scaling by increasing the mode area and the pump power accordingly. In cw operation, more than 8 kW of power were achieved from a multimode (M^2>8) thin-disk laser (TDL) with one single disk as gain medium [7]. Furthermore, up to 4 kW near single fundamental mode operation (M^2>1.38) have recently been demonstrated [7]. In a more complex layout, 30 kW of nearly diffraction-limited output power has been achieved [8] using ten disks in one resonator.

One important advantage of the thin-disk laser concept is the low cavity round-trip nonlinearity which is even more important for ultrafast pulse generation with very high peak power. The most powerful ultrafast laser demonstrated to date is based on a multipass thin-disk amplifier generating an average output power of 1.4 kW at a pulse repetition rate of 300 kHz with 8 ps pulses [9], which has been even improved to 1.9 kW of average power most recently [10]. Regenerative amplifiers based on TDLs have also made large progress in the last few years [11,12]. For even higher megahertz pulse repetition rates modelocked ultrafast thin-disk laser oscillators are very attractive, as they generate hundreds of watts of average power directly from a compact oscillator with excellent beam quality (M^2 = 1) and low-noise properties [13–15].

All of these record-performance high-power thin-disk sources are based on Yb:YAG. Apart from the advantages highlighted above, this gain material exhibits an attractive combination of spectroscopic and thermo-mechanical properties ideally suited for the thin-disk geometry. The high hardness enables high-quality thin-disk preparation. Yb:YAG has good heat-removal capabilities at low doping concentrations and a relatively high absorption cross section, which is beneficial for efficient laser operation with thin gain media. Yb:YAG is easily grown in large sizes using the standard Czochralski method. Furthermore, for ultrafast applications, Yb:YAG offers an attractive combination of high emission cross section and a sufficiently broad bandwidth to support ultrashort high-power pulse durations of down to several 100s of fs with passive modelocking [13,15].

Optics EXPRESS

Further power scaling would benefit from some additional properties. In particular, the disk thicknesses will need to be further decreased for efficient heat removal and reduction of thermal aberrations. This requires high doping concentrations for sufficient absorption [16–18]. The thermal conductivity κ of Yb:YAG, however, drops significantly with increased disk doping concentration (9 W/m/K at 2 at.% and 6 W/m/K at 10 at.% [19]). In recent years, remarkable research efforts were carried out to find new host materials for the Yb ion specifically for high-power operation in the thin-disk geometry [20–23]. A particularly promising alternative is the mixed sesquioxide Yb:Lu_2O_3, which exhibits a thermal conductivity that stays almost constant up to highest doping concentrations (12 W/m/K) [2]. Additionally, its emission spectrum is broader than Yb:YAG's, thus supporting shorter pulse durations [13]. Unfortunately, because Yb:Lu_2O_3's melting temperature is 500°C higher than Yb:YAG's (2450°C versus 1940°C), it can only be grown with the complex and costly heat-exchanger method [2]. Furthermore, its narrow absorption spectrum requires wavelength-stabilized diodes. Therefore, Yb:YAG stays the preferred material in commercial and low-cost applications due to the possibility to grow large crystals in reproducible and excellent optical quality by the well-established Czochralski technique.

In this paper, we investigate the potential of another promising gain crystal for the high-power thin-disk geometry, Yb:$Gd_3Ga_5O_{12}$ (Yb:GGG). Table 1 summarizes the key material properties in comparison to Yb:YAG. The most striking feature of the Yb:GGG gain material is its thermal conductivity κ of 7.8 W/m/K, which remains nearly independent of doping concentration up to >20 at.%, and is higher than Yb:YAG at doping concentrations >4 at.% [19,24,29]. Additionally, the quantum defect of Yb:GGG can be 20% lower than the one of Yb:YAG. The other spectroscopic characteristics of Yb:GGG are similar to Yb:YAG, such as a broadband absorption spectrum, a sufficiently wide emission spectrum, and favorable quenching behavior. The material hardness of Yb:GGG is 7.5 Mohs, which is still sufficiently high for thin-disk preparation and very close to Yb:YAG (8.5 Mohs, Table 1). Furthermore, the low melting temperature of 1750°C and large segregation coefficient of rare earth ions allows for the large-scale Czochralski fabrication method. Diameters as large as 190 mm have already been demonstrated. Therefore, the new gain material Yb:GGG is particularly attractive for further power scaling of thin-disk laser sources, potentially replacing Yb:YAG in the future.

So far, this promising gain material had not been tested in the thin-disk configuration. Results of diode-pumped Yb:GGG were only achieved in the bulk geometry and at moderate power levels <6 W [24,30], both in cw and Q-switched configuration. Here, we present the first demonstration of an Yb:GGG thin-disk laser. With the help of finite-element-method (FEM) simulations we show the advantageous heat-removal capabilities of Yb:GGG over Yb:YAG, resulting in >50% lower temperature rise and thermal lensing for thin Yb:GGG disks compared to Yb:YAG disks. Furthermore, we demonstrate the mechanical suitability of this crystal for all the steps required for thin-disk mounting. In transverse multimode cw operation, we scale the previously achieved output powers up by an order of magnitude to >50 W. Additionally, we compare this performance with an Yb:YAG disk under identical pumping conditions and find similar output characteristics. The equivalent optical performance of the two crystals in combination with the easy growth and the significant thermal benefits of Yb:GGG shows the large potential of high-power thin-disk amplifiers and lasers based on this material, both for industrial and scientific use.

This paper is organized as follows. In section 2 we give an overview of the key parameters of Yb:GGG in comparison to Yb:YAG. We then describe the growth and contacting process of our crystal. Furthermore, we add simulations based on the rate equations for quasi-three-level systems and FEM to demonstrate the thermal-lensing benefits of Yb:GGG over Yb:YAG in future power-scaled thin-disk lasers. Section 3 highlights the results of our high-power lasing experiments. We then summarize our results in the final section 4 and provide an outlook.

Optics EXPRESS

2. Yb:GGG - a promising thin-disk gain crystal for power scaling

2.1 Yb:GGG crystal properties, growth, and thin-disk fabrication

In this chapter, we provide an overview of the most important spectroscopic and thermo-mechanical properties of Yb:YAG and Yb:GGG, in particular for high-power thin-disk laser operation. These parameters are summarized in Table 1.

Gadolinium Gallium Garnet (GGG) crystallizes in the cubic structure in the Ia3d space group, just as YAG. During doping with Yb^{3+} ions, the dopant and the replaced Gd^{3+} ions have the same charge state and comparable ionic radii, therefore the dopants do not disturb the crystal lattice and do not alter the crystal properties [31]. Additionally, thanks to the larger lattice parameter of GGG compared to YAG (12.38 Å versus 12.01 Å), the average distance between Yb ions in GGG crystals is larger than in YAG crystals for the same molar concentration. This reduces non-radiative transition effects such as cooperative luminescence caused by ion-ion interaction and decreases the degree of lattice distortion defects after Yb doping. In particular, this makes the GGG crystal matrix more favorable for high Yb doping levels compared to YAG. Namely, Yb:GGG's high thermal conductivity κ remains nearly independent of doping concentration up to >20 at.%, in contrary to Yb:YAG [19,24].

Thanks to their similar host-crystal structures, the spectroscopic characteristics of Yb:GGG are comparable to Yb:YAG [24,25], see Fig. 1. In particular, both Yb:YAG and Yb:GGG have broadband absorption plateaus around 940 nm, which allow for cost-effective pumping with non-wavelength-stabilized diode arrays. From the zero-phonon line and the maximum emission wavelength it follows that the quantum defect of Yb:GGG can be up to 20% lower than the one of Yb:YAG, resulting in an overall significantly reduced thermal load during lasing.

Table 1. Overview of Yb:GGG crystal properties in comparison to Yb:YAG [1,19,24–28]

	Yb:GGG	**Yb:YAG**
Zero-phonon line *ZPL*	971 nm	969 nm
σ_{abs} (ZPL)	$6.6*10^{-25}$ cm^2	$5.6*10^{-25}$ cm^2
Broadband absorption between	930 nm – 950 nm	930 nm – 950 nm
Peak emission wavelength *EW*	1021 nm	1030 nm
σ_{em} (EW)	$1.9*10^{-24}$ cm^2	$2.0*10^{-24}$ cm^2
$\Delta\lambda_{emission}$ (FWHM at inversion ~10%)	8 nm	7 nm
Quantum defect (rel. to Yb:YAG)	80%	100%
κ (5 at.%)	7.8 W/m/K	7.2 W/m/K
κ (15 at.%)	7.7 W/m/K	5.8 W/m/K
Coefficient of thermal expansion *CTE*	$8*10^{-6}$ K^{-1}	$8*10^{-6}$ K^{-1}
Hardness	7.5 Mohs	8.5 Mohs
Melting temperature	1750°C	1940°C

The Yb:GGG crystal used for our experiments was grown by the Czochralski method. This allows for straightforward and large-scale growth with Iridium crucibles, which could enable large-volume and commercial growth in the future. The polycrystalline Yb:GGG material was synthesized by a conventional solid-state reaction at 1280°C for 48 h. The starting material had an Yb^{3+} concentration of 10 at.% and was melt completely in an Iridium crucible. The single crystal was grown in a RF-induction-heating Czochralski furnace. A pure GGG crystal rod with <111> orientation was used as seed. The pulling and the rotation rates were set to 0.8 mm/h and 15 rpm, respectively. After growth, the obtained crystal was annealed in air at 1400°C for 40 h to release thermal stress.

Optics EXPRESS

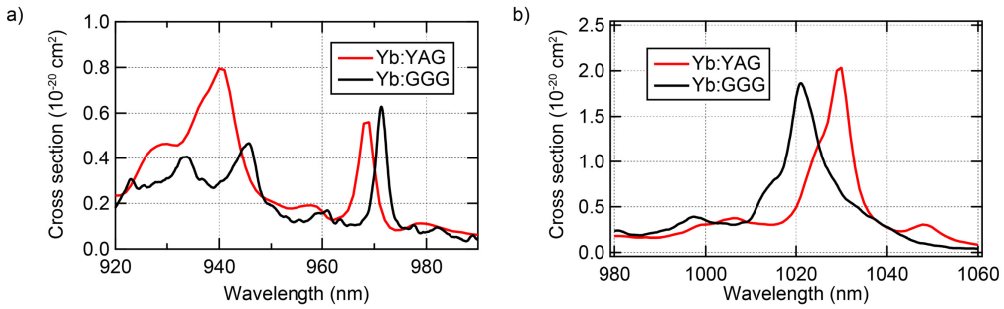

Fig. 1. (a) Absorption and (b) emission cross sections of Yb:GGG [24] in comparison with Yb:YAG [1].

Subsequently, we utilized Yb:GGG's high hardness (7.5 Mohs, comparable to Yb:YAG, see Table 1) to cut the boule and polish it into 95-µm-thin disks with a diameter of 8.5 mm and a <111> orientation. The final resulting Yb concentration was measured by the XRF technique (Rigaku ZSX Primus II) to be 11.9 at.%. Afterwards, the crystal was coated with a highly-reflective coating for the laser and pump wavelength on one side and with an anti-reflective coating on the other side. It was contacted onto a diamond heat sink by Dausinger + Giesen GmbH [see Fig. 2(a) for the contacted disk]. Unfortunately, some scratches were introduced to our disk during the polishing process as shown in Fig. 2(b).

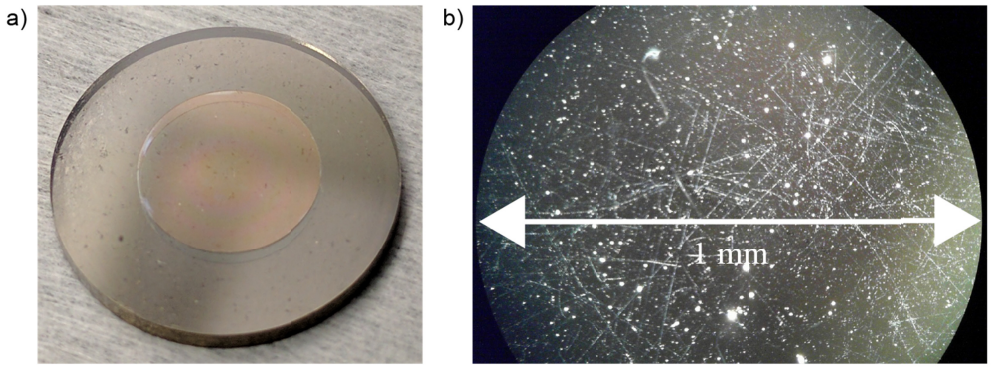

Fig. 2. (a) Yb(11.9 at.%):GGG thin disk after contacting onto the diamond heat sink. (b) Several scratches were introduced to our Yb:GGG disk during polishing. Picture obtained with a dark-field microscope.

2.2 Thermal effects: comparison between Yb:GGG and Yb:YAG

In order to quantify the thermal advantages of Yb:GGG for thin-disk operation, we performed FEM simulations using COMSOL to study the thermal behavior of an Yb:GGG disk. In particular, we investigated the potential thermal-lensing benefit of Yb:GGG compared to Yb:YAG during laser operation based on the key advantage of Yb:GGG crystals to achieve both a high doping concentration and a high thermal conductivity simultaneously.

Increasing pump powers requires thinner disks for efficient heat removal. Decreasing the disk thickness leads to a decrease of the overall optical-to-optical efficiency of the laser [16–18,32] if a constant number of pump passes is used. This performance reduction can be compensated by increasing the disk doping. In the case of Yb:YAG, this results in a decrease of the thermal conductivity κ, whereas for Yb:GGG κ is unaffected by the doping concentration. For thin disks, Yb:GGG's κ is therefore significantly higher than the one of Yb:YAG, leading in return to a heavily reduced temperature rise during high-power thin-disk operation. This directly couples to a lower thermal lensing effect and reduced cavity

Optics EXPRESS

instabilities of Yb:GGG compared to Yb:YAG. In the following, we describe and quantify these benefits in more detail.

Based on the rate equations for quasi-three-level thin-disk laser systems [32], we can simulate the optical-to-optical efficiency of a thin-disk laser in multimode cw operation for both Yb:GGG and Yb:YAG. In our investigation, we assumed a standard 24-pass thin-disk head (also used in our experiments, see Section 3), an output coupler of 10%, and an additional cavity loss of 0.5%. The pump power was set to 400 W, and the pump-spot diameter to 2.6 mm, a typical value for high-power TDLs. For different optical-to-optical efficiencies we can show that thinner disks require a significantly higher doping concentration [Fig. 3(a)]. Without the higher doping concentration both the pump absorption efficiency drops and the laser threshold increases.

For Yb:YAG, the required higher doping concentration for thin disks leads to a significant drop in thermal conductivity κ, whereas for Yb:GGG κ stays practically constant. In Fig. 3(b) we quantified this effect for a constant 65% optical-to-optical efficiency of the TDL. The required doping concentrations for Yb:GGG differ slightly from the ones of Yb:YAG and are not explicitly stated here. We plotted the corresponding thermal conductivities for both crystals, which show a significant drop for Yb:YAG and an almost constant value for Yb:GGG.

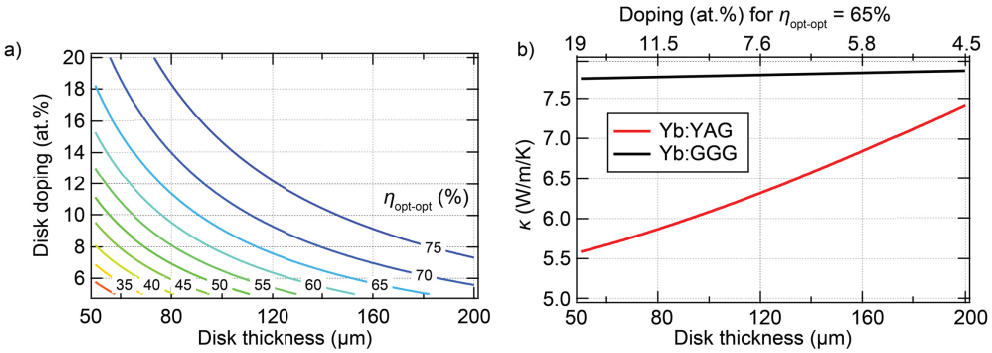

Fig. 3. (a) Simulated optical-to-optical efficiency ($\eta_{opt-opt}$) of a multimode cw Yb:GGG thin-disk laser (TDL) versus the disk thickness and the disk doping, based on the zero-dimensional model [32]. Decreasing the disk thickness requires an increased disk doping to keep a high $\eta_{opt-opt}$. Parameters: material Yb:GGG, V cavity, pump power 400 W, pump-spot diameter 2.6 mm, pump passes 24, cavity losses 0.5%, output-coupling rate 10%. (b) Disk doping (top horizontal axis) required to achieve a $\eta_{opt-opt}$ = 65% as a function of disk thickness (bottom horizontal axis). The resulting thermal conductivity for Yb:YAG drops significantly when going to thinner disks, whereas the one for Yb:GGG stays nearly unchanged.

Keeping the optical-to-optical efficiency constant at 65% [Fig. 3(b)] we simulated with the FEM software COMSOL the maximum disk temperature versus the disk thickness with a pump power of 400 W in laser operation. Here, the main contribution to the thermal load on the disk originates from the quantum defect. Non-radiative decays (e.g. via quenching or impurities) can be neglected for high-power TDL operation far above the threshold with intracavity intensities much higher than the saturation intensity [33,34]. Our radially symmetric 3D FEM model [see Fig. 4(a)] consisted of the disk mounted on a 1.4-mm-thick diamond heat sink, whose back side was set to the fixed cooling temperature of 20°C. The pump-spot diameter was modeled as 2.6 mm on a 10-mm-diameter disk.

The temperature increase relative to the cold disk is shown in Fig. 4(b). At a disk thickness of 200 µm the Yb:GGG disk exhibits 30% lower temperature increase than the Yb:YAG disk, because of its reduced quantum defect and the higher thermal conductivity at the corresponding doping concentrations in the 5-at.% range. Going to thinner disks below 100 µm for further power scaling, Yb:YAG suffers from its strongly decreasing thermal

Optics EXPRESS

conductivity due to increased dopings. In this case, Yb:GGG disks remain at a 50% lower temperature increase compared to Yb:YAG disks.

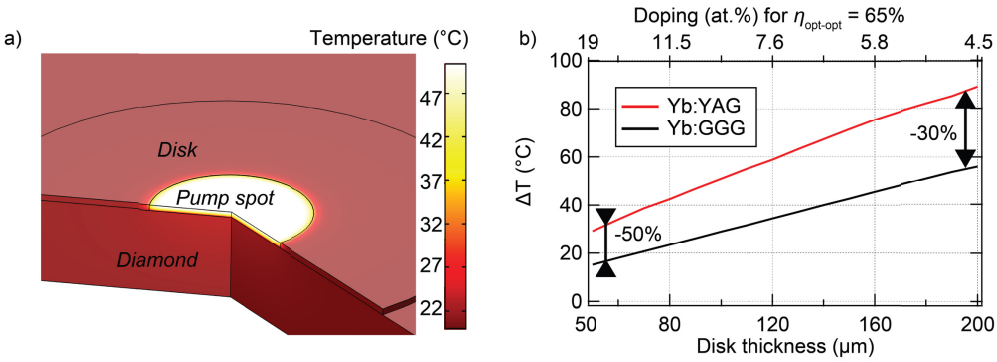

Fig. 4. Example with 400 W of pump power, 2.6 mm of pump-spot diameter, and varying disk thickness, with the disk doping and thermal conductivity as shown in Fig. 3(b) for a fixed 65% optical-to-optical efficiency: (a) Sample image of finite-element-method (FEM) simulations. (b) COMSOL simulations of disk temperature increase ΔT relative to room temperature versus disk thickness. For thinner disks with higher doping concentrations, Yb:GGG potentially has 50% lower ΔT compared to Yb:YAG. Yb:GGG benefits from its reduced quantum defect and high thermal conductivity.

Thermal lensing is an accumulation of several effects, which are directly proportional to the disk-temperature increase [35,36]. Excessive thermal lensing leads to cavity instabilities and mode breakdown [13]. Therefore minimizing this effect is crucial for high-power thin-disk operation, in particular for applications where good beam quality is required. The main contributions to thermal lensing are disk bending and thermo-optic-induced refractive-index changes, where disk bending typically is an order of magnitude stronger [35]. The effective focal power due to disk bending F_{bend} is directly proportional to the temperature increase ΔT and the coefficient of thermal expansion CTE, i.e. $F_{bend} \propto CTE * \Delta T$ [35]. The CTEs of Yb:GGG and Yb:YAG are practically identical (see Table 1), and therefore the difference in F_{bend} only depends on ΔT. Thus, in the configurations as described above the 50% lower temperature increase of the thin Yb:GGG crystal compared to Yb:YAG directly results in a 50% reduced thermal-lensing effect for Yb:GGG.

In conclusion, Yb:GGG disks can be operated in pump-power regimes where Yb:YAG becomes seriously limited because of excessive heating and thermal-lensing effects. Yb:GGG TDLs can potentially be pumped twice as hard as Yb:YAG disks before reaching critical thermally-induced damage or cavity instabilities due to thermal lensing. This is a major advantage for high-power operation, both in laser amplifier and oscillator designs.

3. High-power laser experiments

In order to compare the performance of our Yb:GGG disk (11.9 at.% doping, 95 µm thickness) with a state-of-the-art Yb:YAG crystal, we used a <111>-orientation, 9-mm-diameter, 100-µm-thick Yb(10 at.%):YAG disk manufactured and contacted on diamond by Trumpf.

We set up an experiment to test their lasing performances under similar conditions. We pumped the disks in a 24-pass arrangement using a pump diode around 930 nm to 935 nm, a wavelength region at which both gain crystals exhibit broadband absorption with similar absorption cross sections. Due to the non-optimized pumping wavelength, however, the absorbed pump powers on our disks were ~80%. The pump-spot diameter was 2.6 mm. Both disks were tested in a highly transverse multimode linear resonator using the disk and a curved output coupler (OC, R = –500 mm) as end mirrors. We placed the output coupler at a

Optics EXPRESS

distance of 10 cm from the disk, with OC rates ranging from 0.4% to 1.8% as summarized in Table 2. We measured the beam quality factor M^2 of the output beam to be ~60.

Table 2. The output parameters of Yb:GGG are comparable to the ones of Yb:YAG, showing similar slope efficiencies for different output-coupling (OC) rates.

OC rate	Slope efficiency **Yb:GGG**	Slope efficiency **Yb:YAG**
0.4%	49%	44%
0.9%	57%	58%
1.3%	**67%**	**66%**
1.8%	54%	57%

We achieved the highest optical-to-optical efficiencies of 53% (Yb:GGG) and 55% (Yb:YAG), relative to an absorbed power of 100 W, with an output coupler of 1.3% [Fig. 5(a)]. The corresponding slope efficiencies, relative to the absorbed power, are 67% (Yb:GGG) and 66% (Yb:YAG), see Table 2. These values stand in good agreement with the simulations for quasi-three-level TDL systems [32] as introduced earlier. The resulting maximum output power was 51 W for the Yb:GGG crystal, and 53 W for the Yb:YAG crystal. For these results we calculated [32] the loss of the optical disk for a single pass and obtained <0.2% for both Yb:YAG and Yb:GGG, which are typical values for state-of-the-art coated thin disks with high optical quality. Additionally, we experimentally verified the lower emission wavelength for Yb:GGG compared to Yb:YAG (see Table 1), ultimately decreasing the quantum defect by up to 20%. The comparable cw multimode performance obtained with these two crystals shows the huge potential of Yb:GGG for high-power operation in the thin-disk geometry.

To investigate the thermal behavior, we used a thermal camera (FLIR SC640) to measure the temperature increase of the surface of the disks under pumping in fluorescence mode (i.e. without cavity feedback and lasing conditions). The transverse spatial resolution of our thermal camera measurements was around 250 μm. In general, we expect to find a higher temperature in fluorescence mode of operation than in laser operation due to non-radiative effects such as concentration quenching or growth defects and impurities [33,34]. These non-radiative effects are quantified with the radiative quantum efficiency η_r [33,34], i.e. a high η_r is an indicator for small non-radiative effects. For high-quality crystals, η_r is in the same range for both Yb:YAG and Yb:GGG (~70%-80% for 10-at.%-doped Yb:YAG and Yb:GGG [37]). Using this knowledge and combining it with our COMSOL simulations, we found excellent agreement between measurement and simulation for our Yb:YAG disk [Fig. 5(b)].

In our experiment, we measured an unexpectedly high temperature rise for our Yb:GGG disk, which ultimately led to damage of the disk. The experimental temperature increase corresponds to an increased heat fraction caused by a low η_r of about 50%. It should be noted that in laser operation far above threshold, the non-radiative channels are suppressed in favor of the radiative ones [37], which explains the good optical behavior of our Yb:GGG disk in lasing conditions [Fig. 5(a)].

Optics EXPRESS

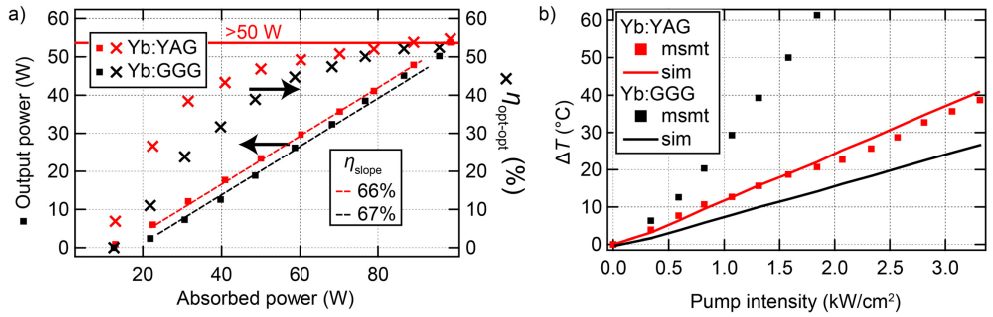

Fig. 5. (a) Multimode cw operation for Yb:GGG and Yb:YAG with an output-coupling rate of 1.3%, reaching >50 W of output power. We achieved slope efficiencies (dashed lines) of 67% (Yb:GGG) and 66% (Yb:YAG). (b) Temperature increase ΔT relative to the cold disk during pumping (only in fluorescence mode of operation, i.e. no lasing). Finite-element-method (FEM) simulations using COMSOL are shown with the solid lines and experimental data with the dots. For Yb:YAG, the simulation fully agrees with the experimental results, however, this is not the case for Yb:GGG. The Yb:GGG crystal becomes unexpectedly hot, which might be due to the low-purity material or defects introduced during growth from the Iridium crucible.

We identified several possible reasons for these significant non-radiative effects of our Yb:GGG crystal. Typically, high-power thin-disk crystals are grown with >5N-purity raw materials. The use of 4N purity in our case led to the inclusion of defects, which might have acted as non-radiative centers. Additionally, Iridium crucibles are known to introduce Fe and Ni impurities to the crystal growth, further decreasing η_r. In the future this problem can be resolved by using high-purity Rhenium crucibles [38].

We are confident that all these issues, as well as the scratches introduced during the polishing process as shown in Fig. 2(b), can be resolved in a straightforward way in the next generation of Yb:GGG thin disks. This will allow us to experimentally benefit from the superior intrinsic heat-removal capabilities of Yb:GGG over Yb:YAG, and push output powers to several 100s of watts. It is worth noting that in this first proof-of-principle experiment, we used a moderate spot size. Using a larger spot size would have most likely resulted in higher power (with damage occurring at a similar pump-power intensity). However, these first results are already an excellent indication of the large potential of this laser material.

4. Summary and outlook

We demonstrated the first Yb:GGG laser in the thin-disk geometry. This material can be easily grown at low temperature and offers beneficial spectroscopic and thermal properties, which makes it a very promising contender to the well-established Yb:YAG for high-power applications. In particular, its quantum defect is 20% lower than the one of Yb:YAG and its high thermal conductivity remains approximately constant even at high doping concentrations.

With the help of finite-element-method (FEM) simulations using COMSOL software we clearly showed the advantageous heat-removal capabilities of Yb:GGG compared to Yb:YAG. They lead to >50% lower temperature rise and thermal lensing for thin Yb:GGG disks compared to Yb:YAG disks for small thicknesses (around 50 µm), where doping concentrations are increased (>15 at.%) in order to maintain a high optical-to-optical efficiency of 65%.

We tested our Yb:GGG thin disk in transverse multimode operation and achieved output powers of >50 W, which is an order of magnitude higher than what was previously demonstrated with this material. We reached a maximum slope efficiency of 67%, which is similar to a state-of-the-art Yb:YAG disk in the same configuration. Despite the material's beneficial thermal properties, we observed a higher operation temperature of this disk

Optics EXPRESS

compared to a similar Yb:YAG disk at the same pumping intensity. This can be explained by growth-induced impurity defects, which can be greatly improved in future growth runs.

Our goal for this paper was to compare this material with a state-of-the-art Yb:YAG disk, therefore we used a doping concentration of 10 at.%. In future experiments, we will increase the doping concentration to >15 at.%, which should support efficient laser operation using thinner disks of around 50 µm with outstanding thermal properties. Additionally, we will investigate the behavior of Yb:GGG in single-fundamental-mode thin-disk operation. We expect this material to to reach several 100s of W cw output powers in the thin-disk configuration in the near future using thinner disks with high doping from improved growth runs. Furthermore, it is also a potentially interesting candidate for high-power picosecond lasers for precision micromachining applications.

Acknowledgments

We acknowledge financial supports received by the Swiss National Science Foundation (SNSF) project grant number 200020-152967, the National Natural Science Foundation of China (Grant Nos. 51227002 and 51323002), and National Key Research and Development Program of China (Grant No. 2016YFB1102201). Additionally, we would like to thank Dr. Frédéric Druon from the Institut d'Optique Graduate School (IOGS) for providing the cross sections for Yb:GGG, and Dr. Christian Kränkel from the Universität Hamburg and Dr. Valentin Wittwer from the Université de Neuchâtel for helpful discussions.

Portions of this work were presented in the Advanced Solid-State Lasers (ASSL) conference in 2016, contribution AM5A.18.